

# 核电 SA508-3 钢大型筒体环焊残余应力分析

迟露鑫<sup>1,2</sup>, 麻永林<sup>2</sup>

(1. 重庆理工大学 材料科学与工程学院, 重庆 400050; 2. 内蒙古科技大学 材料与冶金学院, 包头 014010)

**摘 要:** 为了准确地预测核电 SA508-3 钢的大型筒体环焊温度和残余应力变化规律, 基于 ANSYS 有限元软件, 引入子结构法优化焊接模拟过程, 并比较模拟结果与试验数据。结果表明, 文中采用的计算方法成功地模拟了更加接近真实的筒体环焊过程, 且模拟结果与实测值基本吻合; 焊缝上所有节点的热循环曲线相似, 热影响区的模拟宽度为 4 mm 左右; 筒体外表面焊缝中心线上任意节点的残余应力大小相近, 仅在靠近筒体外表面焊缝中心线附近存在一定的轴向压应力, 其它区域大部分为拉应力, 环向保持较高的拉应力; 筒体焊后产生内凹残余变形; 结果可为分析大型筒体环焊残余应力提供参考数据。

**关键词:** SA508-3 钢; 环焊缝; 子结构; 残余应力; 数值模拟

**中图分类号:** TG113 **文献标识码:** A **文章编号:** 0253-360X(2013)08-0085-04



迟露鑫

## 0 序 言

研究表明<sup>[1]</sup>, 焊接时, 瞬时高温在焊缝及其附近区域产生不均匀的温度梯度分布, 冷却后形成比较复杂的残余应力和变形, 直接影响到焊件的承载能力和结构稳定性。大型核电压力容器主焊缝(纵焊和环焊)焊接是制造这类高压容器的关键工序。在能够准确计算筒体纵向焊接过程的基础上, 模拟筒体环焊焊缝及其附近区域的残余应力状态及分布规律显得尤为重要。

近年来, 随着计算机配置的不断提高, 理论知识的充实, 国内外很多学者利用有限元模拟了钢管的焊接过程, 计算结果与试验数据很好地吻合<sup>[2-4]</sup>。然而目前模拟计算方法主要针对一些小的或者简单的薄壁筒体构件, 对于多层多道焊接过程数值模拟, 文献[5, 6]采用有限元理论研究焊接过程中焊缝填充问题, 模拟结果与试验数据非常吻合, 为研究厚壁焊件的数值模拟提供理论指导。目前, 针对核电 SA508-3 钢筒体环向焊接过程数值模拟还未见相关的文献报道, 因此, 采用 ANSYS 有限元软件, 引入子结构法优化 SA508-3 钢筒体环向焊接模拟过程, 以了解焊接过程中温度及焊后残余应力变化规律, 并将模拟结果与试验数据对比分析, 结果可为分析大

型筒体环焊残余应力提供参考数据, 也为该材料的进一步应用打下基础。

## 1 有限元模型的建立

### 1.1 试验材料

试验用母材为某公司提供的铸态 SA508-3 钢, 其化学成分如表 1 所示。

表 1 SA508-3 钢的化学成分(质量分数, %)

Table 1 Chemical compositions of SA508-3 steel

C	Si	Mn	Ni	Mo	Cr	Fe
0.18	0.17	1.40	0.79	0.51	0.14	余量

### 1.2 焊接工艺

研究对象是将直径为 3 000 mm, 厚度为 20 mm, 长度为 1 000 mm 的两个筒体沿着圆周方向进行埋弧对接焊, 下坡口 7 mm, 上坡口 12 mm, 共焊 4 层, 埋弧自动焊的前 2 层每层 1 道, 其余为每层 2 道, 共 6 道次, 焊接顺序为道次 1 ~ 道次 6。焊接参数: 电流 520 ~ 580 A, 电压 30 ~ 33 V, 焊接速度 300 ~ 400 mm/min, 焊丝直径 4 mm。根据 SA508-3 钢的焊剂与焊丝配合原则, 试验采用焊剂 AT-SJ613HIC (B) 与焊丝 AT-J507HIC (A)。

### 1.3 有限元数值模拟模型

建立筒体环焊三维有限元模型, 采用热-应力间接耦合的计算方法, 即先进行温度场求解, 再把温度

场分析结果作为应力场分析的载荷来实现两个场的耦合计算。因此,温度场和应力场的有限元模型是同一个模型,如图 1 所示。

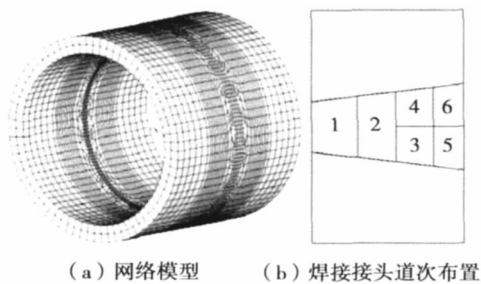


图 1 有限元模型

Fig. 1 Model of finite element

#### 1.4 有限元算法的程序优化设计

为了实现大型筒体环焊数值模拟,采用有限元子结构法,即利用 ANSYS 编写子结构程序。将焊缝及近焊缝区受温度影响比较大的区域,模拟计算为非线性,远离焊缝受温度影响比较小的位置认为线性计算,因此,把筒体划分为焊缝区、过渡区和远离焊缝区域共三部分。首先仅将待焊道次的焊缝区域单元和过渡区域单元作为子结构进行焊接过程数值模拟,当该道次焊缝焊接模拟结束后,退出子结构,再模拟整个筒体冷却过程,都计算结束后,重新进入子结构,进行下一道次往复循环模拟计算。

由相同配置的计算机模拟结果表明,采用子结构法模拟筒体环向焊接过程,实现了热源动态的准确加载,更加接近真实的筒体环向焊接过程,这在尽量不影响焊接模拟精度的前提下,减小了大型筒体环向焊接的线性单元重复计算,优化了焊接模拟过程,计算效率提高了 43 %。

## 2 温度场模拟与分析

焊接温度场的准确计算是焊接冶金分析、焊接应力和变形分析以及焊接质量控制的前提<sup>[7]</sup>,由于在多层多道焊接过程中,工件经历多次焊接热循环,温度场变化情况非常复杂。因此,所选择的路径尽可能全面分析温度场模拟结果,如图 2 所示。在筒体任选一位置做垂直焊缝的截面 A,路径 1 是沿着焊接方向的筒体焊缝外表面中心线,路径 2 是筒体截面 A 上沿着焊缝厚度方向的焊缝宽度中心线,路径 3 和路径 4 分别是筒体截面 A 上垂直焊缝及近焊缝区域的焊缝外表面线及中部线。

图 3 为不同路径的热循环曲线。由图 3a、b 可

知,沿着同一条焊缝上和沿着焊缝厚度方向上的节点热循环曲线相同,只是到达峰值温度的时间不同,即焊缝上任意节点经历相似的热循环曲线,不随位置的变化而变化,峰值温度在 1 910 ℃ 左右,高温(温度超过 1 500 ℃)大约停留 3 s。由图 3c、d 可知,到焊缝中心线不同距离节点的热循环曲线基本相似,随着与热源距离的依次增大,热源的作用逐渐减弱,其温度峰值也就逐渐减小,对材料性能影响也逐渐减小,如节点 g 到热源的距离为 11 mm,其峰值温度 720 ℃,节点 n 到热源的距离为 7 mm,其峰值温度为 892 ℃,结合 SA508-3 钢的 AC1(717 ℃),可知,筒体环焊数值模拟的热影响区宽度为 4 mm 左右。

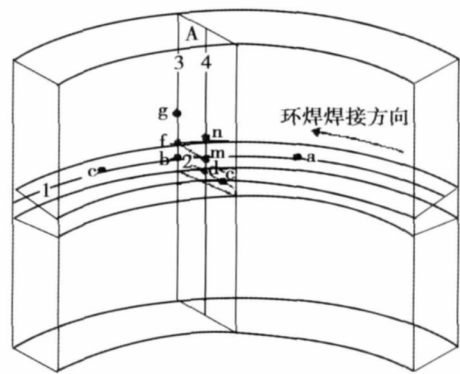


图 2 路径布置图

Fig. 2 Path layout diagram

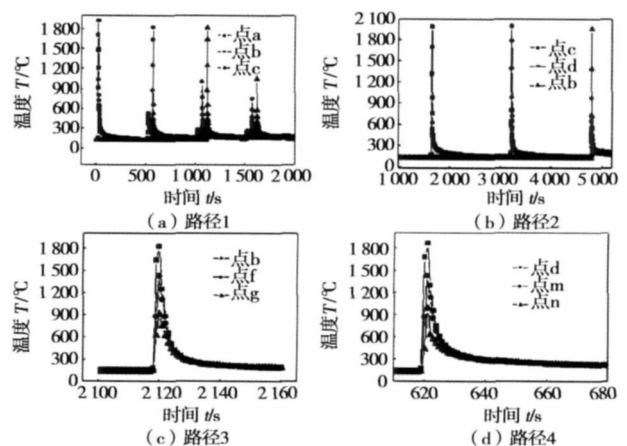


图 3 不同路径的热循环曲线

Fig. 3 Thermal circling curves of different paths

## 3 残余应力场模拟与验证

#### 3.1 边界条件及初始条件

筒体环焊温度场数值模拟的初始温度为预热温

度  $121\text{ }^{\circ}\text{C}$ 。焊接过程中,焊件与外界同时存在对流和热辐射换热,因此,筒体内外表面均施加边界条件,对流系数取  $10\text{ W}/(\text{m}^2\text{K})$ 。在间接耦合应力场分析中,在筒体环向对接焊远离焊缝一端的四个方向上各取一点进行  $x, y, z$  三个方向的全约束控制。

### 3.2 筒体热变形

筒体环向焊接结束,冷却到室温后的热变形如图4所示,为了使显示效果更加清楚,将筒体总变形云图放大20倍。

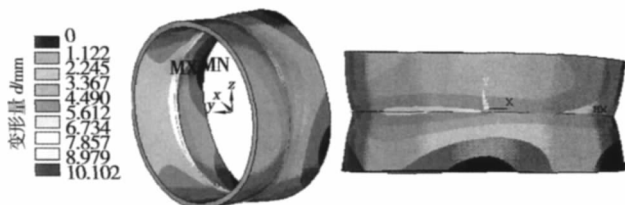


图4 热变形

Fig. 4 Thermal deformation

由图4可知,模型焊接结束冷却到室温后,筒体环焊残余变形不仅发生面内变形的纵向收缩和横向收缩,还有面外变形的角变形。因为焊缝在直径方向收缩具有较大的自由度,使焊缝中心产生了环向残余拉应力,造成环向焊缝向内收缩,便在焊缝及近焊缝区域形成了内凹的残余变形,引起较大的“弯曲应力”,在筒体上形成了一条“束带”,最大值内凹残余变形为  $10.102\text{ mm}$ ,位于筒体焊缝内表面,这就降低了筒体结构的承载能力。

### 3.3 残余应力曲线分析

为了获得较为详细的筒体环焊焊缝及近焊缝区域残余应力变化规律,选择模型上1、2、3和5共四条路径分析焊接残余应力变化规律,结果见图5。

图5a为筒体外表面焊缝中心线上的残余应力,由于焊接稳定阶段的温度场分布相同,使得焊缝中心线上任意位置的节点残余应力在沿着焊接方向的大小及变化规律相近。由于焊接强烈弯曲效应的叠加,使先焊焊道承受拉伸,后焊焊道承受压缩,同时由于在焊缝根部的角收缩倾向较大,所以在角收缩受到约束,则表现为横向压缩<sup>[9-10]</sup>,如图5b为沿着焊缝厚度方向的轴向、环向残余应力,在靠近筒体外表面焊缝及附近存在一定的轴向压应力,其它区域大部分为轴向拉应力。焊缝表面和心部散热条件不同,造成了筒体焊缝外表面和内表面残余应力方向和数值大小的不同,筒体外表面焊缝中心附近的轴向残余应力为压应力且最大值为  $55\text{ MPa}$ ,而筒体内表面焊缝中心附近为轴向拉应力且最大值为  $306\text{ MPa}$ 。

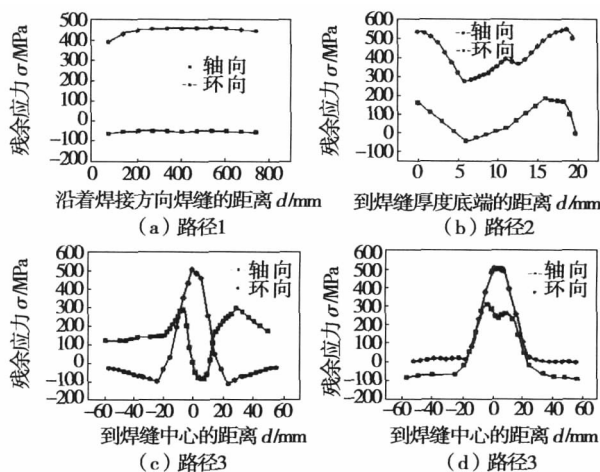


图5 不同路径的残余应力曲线

Fig. 5 Residual stress curves of different paths

MPa,环向一直保持较高的拉应力,见图5c、d,因此,产生弯曲应力而使焊缝向筒体内侧弯曲。

### 3.4 焊接模拟计算与试验验证

为了验证模拟结果是否准确,比较相同焊接工艺条件下SA508-3钢的埋弧焊接模拟值与实测值。选择路径1上的1个节点利用热电偶的方法测试焊接过程热循环曲线。焊接结束,焊件冷却到室温后,利用盲孔法测量路径1上焊缝及其附近位置的特征点残余应力,为了排除人为因素产生的误差,选择与路径1平行的两条路径进行残余应力测量,整理数据,将测试数据与模拟结果对比,见图6和图7。

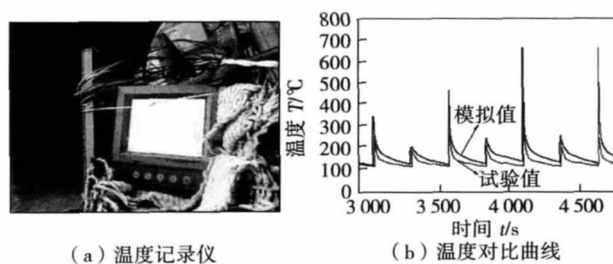


图6 温度场对比曲线

Fig. 6 Comparison curves of temperature field

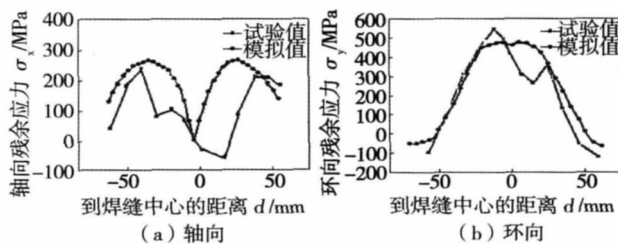


图7 残余应力对比曲线

Fig. 7 Comparison curves of residual stress

由图 6 可知,在所选择的焊接时间段内,实测的特征点峰值温度与模拟峰值温度基本吻合,虽然模型冷却到 200 ℃ 以下时的温度存在一定的差异,但已经对焊接组织的影响较弱,因此,热模型和计算方法较正确,可以进行应力场模拟计算。

由图 7 可知,模拟的轴向残余应力大部分数据比实测值略大,这是由于工件焊后变形,残余应力得到一定的释放以及测量过程的误差等影响,而环向残余应力与实测值比较接近。说明建立的大型筒体环向焊接模型比较合理,采用有限元预测焊接过程的方法是可行的,可为实际焊接工作提供指导。

## 4 结 论

(1) 由相同配置的计算机模拟结果表明,采用子结构模拟焊接过程,更加接近真实的筒体环向焊接过程,这在尽量不影响焊接模拟精度的前提下,计算效率提高了 43 %。

(2) SA508-3 钢筒体环焊模拟结果表明,筒体外表面焊缝中心线上任意节点的残余应力大小相近,仅在靠近筒体外表面焊缝中心附近存在一定的轴向压应力,其它区域大部分为拉应力,环向保持较高的拉应力;筒体焊后产生内凹残余变形。

(3) 比较 SA508-3 钢焊接模拟值与实测值,模拟特征点峰值温度与实测峰值温度基本吻合;模拟的轴向残余应力大部分数据比实测值略大,环向残余应力与实测值比较接近。说明建立的大型筒体环向焊接模型比较合理,采用有限元预测焊接过程的方法是可行的,可为实际焊接工作提供指导。

## 参考文献:

- [1] 徐伟锋,刘合金,朱宏强. 2219 铝合金厚板搅拌摩擦焊接温度场数值模拟[J]. 焊接学报,2010,31(2): 63-66.  
Xu Weifeng, Liu Hejin, Zhu Hongqiang. Numerical simulation of thermal field of friction stir welded 2219 aluminum alloy thick plate[J]. Transactions of the China Welding Institution, 2010, 31(2): 63-66.

- [2] 董俊慧,林 燕. 数值计算模拟工艺参数对管道环焊缝残余应力的影响[J]. 焊接学报,2008,29(3): 121-124.  
Dong Junhui, Lin Yan. Effect of simulated welding parameters on pipe girth weld residual stresses[J]. Transactions of the China Welding Institution, 2008, 29(3): 121-124.
- [3] Dean Deng. Predicting welding residual stresses in a dissimilar metal girth welded pipe using 3D finite element model with a simplified heat source[J]. Nuclear Engineering and Design, 2011(241): 46-54.
- [4] 李亚娟,李午申. X80 圆筒线钢环焊缝接头残余应力的数值模拟[J]. 焊接学报,2010,31(6): 97-101.  
Li Yajuan, Li Wushen. Numerical simulation on welding residual stresses of X80 pipeline girth weld joint[J]. Transactions of the China Welding Institution, 2010, 31(6): 97-101.
- [5] Gao Jiashuang, Yang Jianguo, Fang Hongyuan, et al. A method to simulate multilayer welding process: Node dynamic relaxation method[J]. China Welding, 2009, 18(3): 37-41.
- [6] Fang Hongyuan, Wang Tao, Hu Junfeng, et al. Node dynamic relaxation method: principle and application[J]. Frontiers of Materials Science, 2011, 5(2): 179-195.
- [7] 方臣富,王海松,刘 川,等. 缆式焊丝 CO<sub>2</sub> 气体保护焊接头残余应力高效数值计算和试验[J]. 焊接学报,2012,33(5): 17-20.  
Fang Chenfu, Wang Haisong, Liu Chan, et al. Efficient numerical simulation and experimental study on residual stress induced by GMAW with cable-type wire[J]. Transactions of the China Welding Institution, 2012, 33(5): 17-20.
- [8] 杨秀芝,余圣甫,姚润钢. 双丝焊温度场算法的程序优化设计[J]. 焊接学报,2010,31(10): 53-56.  
Yang Xiuzhi, Yu Shengfu, Yao Runzhi. Optimiazation design of twin-wire welding temperature field algorithm procedures[J]. Transactions of the China Welding Institution, 2010, 31(10): 53-56.
- [9] 郭桂芳,陈芙蓉,李林贺. 7075 铝合金电子束焊接温度场数值模拟[J]. 焊接,2006(3): 28-30.  
Guo Guifang, Chen Furong, Li Linhe. Numerical simulation of temperature field of electron beam welding for 7075 alloy[J]. Welding & Joining, 2006(3): 28-30.
- [10] 方洪渊. 焊接结构学[M]. 北京: 机械工业出版社,2009.

作者简介: 迟露鑫,女,1979 年出生,博士研究生. 主要从事焊接结构质量和残余应力数值模拟方面的科研工作. 发表论文 7 篇.  
Email: chiluxin200195@163.com

ty of Kentucky , Lexington 40506 , USA) . pp 71 – 75

**Abstract:** A novel and highly effective consumable double electrode gas metal arc welding method was introduced. However , the coupled arc and welding process were very unstable in practice and led to serious defects in the weld bead. A new double closed-loop control plan was proposed and simulated after analysis of the relationship between welding parameters to control the bypass arc through the bypass feed speed and control the motherboard current through the bypass current. Then the experiments with this plan were carried out using rapid prototyping and Matlab/Simulink. The results show that the stable welding process and motherboard current could be achieved , and the welds with less defects and good appearance were also obtained.

**Key words:** consumable double electrode gas metal arc welding; control; simulation; welding experiment

**A novel method for measuring the weld property of tailor welded blanks based on DIC** CHEN Shuisheng<sup>1</sup> , LIN Jianping<sup>2</sup> ( 1. School of Mechanical and Power Engineering , Henan Polytechnic University , Jiaozuo 454000 , China; 2. College of Mechanical Engineering , Tongji University , Shanghai 201804 , China) . pp 76 – 80

**Abstract:** A novel method , weld division method , was proposed to measure the mechanical properties of the weld zone in tailor welded blanks ( TWBs) . The weld zone was divided into the weld and heat affected zone according to the different minor strains in the direction perpendicular to the weld. The digital image correlation technology was employed to capture the strain field in the TWBs surface when the weld failure occurred. A theoretical model was established to calculate the strength coefficient K and strain-hardening exponent n based on the previously achieved minor strain. To verify the proposed method , the curves of load vs. displacement were produced using finite element method by implementing the parameters from the division method , during uniaxial test of longitudinal weld in laser TWBs. Compared with the results from the rule of mixtures , those from the division method were closer to the experimental results , which indicates that the division method was more accurate.

**Key words:** tailor welded blanks ( TWBs) ; digital image correlation; weld; division method

**Effect of surface nanocrystallization on stress corrosion cracking behaviors of X80 pipeline steel** WANG Bingying , MIAO Yan , ZHOU Shengnan , HOU ZhenBo ( College of Mechanical and Electrical Engineering , China University of Petroleum , Qingdao 266580 , China) . pp 81 – 84

**Abstract:** Surface nanocrystallization of X80 pipeline steel was realized by ultrasonic surface rolling processing ( USRP) , and the microstructure of the steel surface was analyzed with optical microscope and transmission electron microscopy. The effects of USRP on the stress corrosion behavior of X80 pipeline steel in NS4 solution was investigated through the slow strain rate tensile tests ( SSRT) and scanning electron microscopy. The results show that the USRP refined the grains in the X80 pipeline steel surface to nanometer level. With the negative shift of applied potential , the fracture time , section shrinkage and strain of

the X80 pipeline steel significantly decreased , which suggested that the susceptibility to stress corrosion cracking ( SCC) increased , and the fractured surface revealed transgranular with the feature of quasi-cleavage. Surface nanocrystallization could extend the fracture time and enhance the stress corrosion resistance of X80 pipeline steel.

**Key words:** surface nanocrystallization; X80 pipeline steel; stress corrosion; slow strain rate tensile tests ( SSRT)

**Analysis of residual stresses on large-scale wall pipe circular weld of SA508-3 steel for nuclear power** CHI Luxin<sup>1,2</sup> , MA Yonglin<sup>2</sup> ( 1. College of Materials Science and Engineering , Chongqing University of Technology , Chongqing 400050 , China; 2. College of Material and Metallurgy , Inner Mongolia University of Science and Technology , Baotou 014010 , China) . pp 85 – 88

**Abstract:** The ANSYS software and substructure method were used to optimize welding procedure to accurately predict the distribution of welding temperature and residual stress in large-scale pipe of SA508-3 steel for nuclear power. Comparing the simulated and experimental results , it was found that the computation method could successfully simulate the real welding process , and the calculated values agreed well with the measured ones. The thermal cycle curves of all nodes on the weld were similar , the simulated width of heat affected zone was about 4 mm. The residual stress values of arbitrary nodes in the weld centerline on outer surface of pipe were close to each other , however , axial compressive stress only occurred near the weld centerline on outer surface of pipe , tensile stress appeared in other areas with higher value in the circular direction. The pipe had a concave residual deformation after welding. The results could provide theoretical guidance for analyzing the residual stresses in girth welding of large scale pipe.

**Key words:** SA508-3 steel; circular weld; substructure; residual stress; numerical simulation

**Fuzzy comprehensive assessment of prototyping quality for strip cladding based on MATLAB-FIS** GUO Xiao , XU Kai , ZOU Liwei ( Harbin Welding Institute , China Academy of Machinery Science & Technology , Harbin 150028 , China) . pp 89 – 91 , 100

**Abstract:** Fuzzy analytical hierarchy process was employed to establish fuzzy comprehensive assessment model of prototyping quality for strip cladding with bead thickness , width , edge contact angle and straightness. The weight coefficient of each evaluation indicator was determined by constructing fuzzy consistent judgment matrix. Combined with practical welding experiments , the membership function was determined. Based on MATLAB-FIS , the calculation was carried out , and the established fuzzy comprehensive assessment model was verified by designed experiments.

**Key words:** strip cladding; prototyping quality; fuzzy assessment; analytical hierarchy process

**Non-linear continuum fatigue damage model of TC4 titanium alloy welded joints** LIN Youzhi<sup>1</sup> , FU Gaosheng<sup>1,2</sup> , LI Lei<sup>3</sup> , CHEN Jianhong<sup>3</sup> ( 1. Machine and Electronics Engineering